Published in final edited form as:
Biol Psychiatry. 2009 April 15; 65(8): 680–690. doi:10.1016/j.biopsych.2008.10.039.

Degradation of Association and Projection White Matter Systems in Alcoholism Detected with Quantitative Fiber Tracking

Adolf Pfefferbaum, **Margaret Rosenbloom**, **Torsten Rohlfing**, and **Edith V. Sullivan**
From the Neuroscience Program (AP, MR, TR), SRI International, Menlo Park; and Department of Psychiatry and Behavioral Sciences (AP, MR, EVS), Stanford University School of Medicine, Stanford, California

Abstract

Background—Excessive alcohol use can cause macrostructural tissue shrinkage with regional preference for frontal systems. The extent and locus of alcoholism's effect on white matter microstructure is less known.

Methods—Quantitative fiber tracking derived from diffusion tensor imaging (DTI) assessed the integrity of samples of 11 major white matter bundles in 87 alcoholics (59 men, 28 women) and 88 healthy control subjects (42 men, 46 women). Fiber integrity was expressed as fractional anisotropy (FA) and apparent diffusion coefficient (ADC), quantified separately for longitudinal diffusivity (λL), a putative index of axonal integrity, and transverse diffusivity (λT), a putative index of myelin integrity.

Results—Alcoholism affected FA and diffusivity, particularly λT, of several fiber bundles. Frontal and superior sites (frontal forceps, internal and external capsules, fornix, and superior cingulate and longitudinal fasciculi) showed greatest abnormalities in alcoholics relative to control subjects. More posterior and inferior bundles were relatively spared. Lifetime alcohol consumption correlated with regional DTI measures in alcoholic men but not women. When matched for alcohol exposure, alcoholic women showed more DTI signs of white matter degradation than alcoholic men in several fiber bundles. Among all alcoholics, poorer performance on speeded tests correlated with DTI signs of regional white matter degradation.

Conclusions—This survey of multiple brain fiber systems revealed a differential pattern of alcoholism's effect on regional FA and diffusivity with functional consequences attributable in part to compromised fiber microstructure with prominence in signs of myelin degradation. Sex-based differences suggest that women are at enhanced risk for alcoholism-related degradation in selective white matter systems.

Keywords

Alcoholism; brain; diffusion; DTI; fiber tracking; sex differences; white matter

In vivo magnetic resonance imaging (MRI) studies of chronic alcoholism commonly report smaller volumes of gray matter (1–6) and white matter (3,5,6) in the cerebral cortex than

Address reprint requests to Edith V. Sullivan, Ph.D., Department of Psychiatry and Behavioral Sciences, Stanford University School of Medicine (MC5723), 40.T Quarry Road, Stanford, CA 94305-5723; E-mail: edie@stanford.edu.

None of the authors have biomedical financial interests or other potential conflicts of interest relevant to the subject matter of this article.

Supplementary material cited in this article is available online.

normally expected for any given adult age. Whether women are more vulnerable to the deleterious effects of chronic heavy alcohol use than men is controversial (7). Several studies have reported comparable deficits, relative to same-sex control subjects, in alcoholic men and women despite lower alcohol consumption in the women. Such evidence derives from MRI volumetric studies of cortical white and gray matter and cerebro-spinal fluid (CSF) (8), the corpus callosum (9), and hippocampal volumes (10). Other studies found that men had greater abnormalities than women in size of the lateral ventricles, cortical gray matter (11) and white matter, corpus callosum, and pons (12), once differences in intracranial volume, age, and amount of alcohol drunk in their lifetime were taken into account.

Structural MRI studies have shown that white matter subjacent to the cortex, corpus callosum (9,13,14), and pons (15–17) is affected in terms of macrostructural volume deficits in uncomplicated alcoholism. Magnetic resonance (MR) diffusion tensor imaging (DTI) has revealed evidence for microstructural disruption of white matter in alcoholic men and women, even in regions appearing normal on conventional volume imaging (13,18). Chronic heavy alcohol use also disrupts white matter microstructure as manifest by abnormally low fractional anisotropy (FA) both in localized regions of white matter, such as the corpus callosum and centrum semiovale (13,18,19), and also widely distributed throughout the cortex (20) or in right hemisphere white matter tracts linking prefrontal and limbic systems (21). In addition to assessing regional samples of white matter, such as the corpus callosum and its segments or cortical white matter, DTI can provide visual depictions of white matter fiber systems (22–24), which can be measured with quantitative fiber tracking (25,26). An advantage of quantitative fiber tracking is that DTI metrics are derived only from fibers identified in a region of interest, be they more or fewer in one group compared with another, and no contribution is made from nonfiber signal in the region of interest. Using such a method, Chanraud *et al.* (27) found that detoxified alcoholics had 18% fewer fibers per unit volume of white matter in tracts between the midbrain and pons but not between midbrain and thalamus and that the fiber deficit was predictive of poorer performance on a test of mental flexibility.

Here, we used quantitative fiber tracking to examine regional variation in alcoholism's effect on fiber quality of multiple major association and projection tracts and to investigate sex differences in vulnerability to the effects of chronic heavy alcohol use. Diffusion tensor imaging metrics included FA and apparent diffusion coefficient (ADC) decomposed into two components: longitudinal (axial) diffusivity (λL), which can be altered with disruption of axonal integrity and axonal deletion, and transverse (radial) diffusivity (λT), which increases selectively with decline in myelin integrity (28–31). Breakdown of the myelin sheath with aging or disease (32) can result in increases in extracellular fluid, increased transverse diffusivity, and decreased difference between longitudinal and transverse diffusivity (30,31), as well as decreased FA. We also tested the functional relevance of DTI metrics by correlating them with tasks assessing psychomotor speed, attention, incidental memory, and static balance.

Methods and Materials

Participants

Data were combined from two studies on alcoholism (13,20,33–36). Extensive clinical and demographic descriptions and analysis appear elsewhere (37,38). Control data were from men and women who matched the alcoholic groups herein in age range (39). Demographic data of the 175 men and women in the current analysis appear in Table 1.

Participants with alcoholism were recruited by referral from outpatient substance abuse treatment centers. Informed consent followed procedures approved by the Institutional Review Boards of SRI International and Stanford University.

Clinical Evaluation

Study criteria were based on the Structured Clinical Interview for DSM-IV (SCID) (40), administered by clinical psychologists to all subjects. Prospective subjects meeting lifetime criteria for schizophrenia or bipolar disorder or for nonalcohol substance dependence or abuse within the prior 3 months were excluded, as were prospective control subjects meeting DSM-IV criteria for any Axis I disorder. All alcoholics met DSM-IV criteria for alcohol dependence. Global Assessment of Functioning (GAF) was derived from the SCID (41). All subjects were human immunodeficiency virus (HIV) negative either by self-reported medical history or blood test. Autobiographical history of alcohol consumption (5,42,43) yielded quantitative lifetime consumption of alcohol and time since last drink. Interviews and questionnaires assessed current depression symptoms using the Beck Depression Inventory-II (BDI-II) (44); socioeconomic status (SES) using a two-factor scale based on education and occupation (45); handedness (46); history of smoking (current, past, or never); and body mass index (BMI) height cm/weight kg^2) (Table 1).

Groups differed in socioeconomic status, education, BDI-II score, GAP rating, and lifetime alcohol consumption. Only the alcohol consumption variable showed a group by sex interaction: alcoholics drank more than control subjects, and alcoholic men had drunk almost twice as much as the alcoholic women over their lifetime. Alcoholic men and women were not significantly different from each other in age, education, handedness, socioeconomic status, age of onset of alcoholism, length of illness, or current depressive symptoms. Men had been sober for a shorter time before examination (average 3 months for men, 6 months for women). Men were overrepresented in the alcoholic group. More alcoholics than control subjects were smokers; this difference was salient in women.

Image Acquisition Protocol

Imaging was performed on a 1.5 Tesla GE clinical whole body system (General Electric, Milwaukee, Wisconsin). A dual-echo fast spin-echo (FSE) coronal structural sequence was acquired (47 contiguous, 4 mm thick slices; repetition time [TR]/echo time [TE]1/TE2 = 7500/14/98 msec; matrix = 256 × 192). Diffusion tensor imaging was performed with the same slice location parameters as the dual-echo FSE, using a single-shot spin-echo echo-planar imaging technique (47 contiguous, 4 mm thick slices, TR/TE = 10,000/103 msec, matrix = 128 × 128, in-plane resolution = 1.875 mm^2, b-value = 860 sec/mm^2). Diffusion was measured along six noncollinear directions (number of excitations [NEX] 6) with alternating signs to minimize the need to account for cross-terms between imaging and diffusion gradients (47). For each slice, six images with no diffusion weighting (b = 0 sec/mm^2) were also acquired.

Image Processing

The structural data were passed through the FSL Brain Extraction Tool (http://www.fmrib.ox.ac.uk/fsl) (48) to extract the brain. Eddy current-induced image distortions in the diffusion-weighted images for each direction were minimized by alignment with an average made of all 12 diffusion-weighted images using a two-dimensional (2-D) six-parameter affine correction on a slice-by-slice basis (49). The DTI data were then aligned using the FSE data by a nonlinear three-dimensional (3-D) warp (third-order polynomial), which provided in-plane and through-plane alignment. On a voxel-by-voxel basis, FA and ADC, the latter decomposed into its longitudinal and ($\lambda L = \lambda_1$) and transverse ($\lambda T = [\lambda_2 +$

$\lambda_3]/2$) components, were computed. Fractional anisotropy ranged from 0 to 1, and diffusivity was expressed in units of 10^{-6} mm^2/sec.

Warping to Common Coordinates

To achieve common anatomical coordinates across subjects, a population-average FA template (39) was constructed from the FA data of 120 control subjects (20–81 years old) with group-wise affine registration (50) followed by iterative nonrigid averaging (51,52), Each subject's FA dataset was registered to the population FA template with a nine-parameter affine transformation followed by nonrigid alignment using a multilevel, third-order B-spline with 5-mm final control point spacing (51,53).

Fiber Tracking

The fiber tracking routine (22,54) applies a target-source convention that restricts the fibers to ones originating in source voxels and passing through target voxels (for details, see 39). Fiber tracking bundle targets were identified on the population FA template in white matter locations (39): fornix, internal capsule, external capsule, frontal forceps, occipital forceps, superior cingulate, inferior cingulate, superior longitudinal fasciculus, inferior longitudinal fasciculus, pontocerebellar tract, and cerebellar hemispheres (Figure 1). Sources were defined as 5.625 mm thick planes placed as follows: frontal and occipital forceps and superior and inferior cingulate; superior and inferior longitudinal fasciculi source planes were placed 5.625 mm anterior and 5.625 mm posterior to the frontal and occipital forceps; internal and external capsule source planes were placed 5.625 mm superior and 5.625 mm inferior to these targets. Cubes surrounding the fornix, pontocerebellar tracts, and cerebellar hemispheres served as sources for these targets. For each subject, the targets and sources were mapped from the population FA template to that subject's native image space and passed to the fiber tracking routine. This process compensates for brain size differences among individuals, as those with smaller brains will have smaller regions of interest (ROIs) and those with larger brains will have larger ROIs. Tracking parameters specified minimum FA (.17) and threshold (.125), maximum voxel-to-voxel coherence, and minimum (11.25 mm) and maximum (45 mm) fiber length, with essentially no limit on the number of fibers (other than the number of source pixels), which we refer to as fiber bundles. For each fiber bundle, the mean FA and ADC, λL, and λT were the units of analysis. After fiber detection, the fiber locations were transformed back to common coordinates (i.e., population FA template space) for display.

The accuracy of the landmark target identification depends on the accuracy with which the registration maps points identified in the atlas FA image onto anatomically corresponding points in each of the subject images. If this registration is perfect, then identification of landmarks in the subject images will be perfectly consistent with the landmarks defined in the atlas and also perfectly consistent among all subject images. Thus, we performed a consistency analysis as an estimate of registration accuracy. The landmarks were mapped from the atlas to each subject via the forward atlas-to-subject registration and then back to the atlas (subject-to-atlas inverse) using an independently computed registration in the opposite direction. The Euclidean distance between the original atlas landmark and the same landmark mapped to the subject and back is a measure of how consistently two independent registrations (here, one in each direction) map the landmarks between images. Using this procedure, the mean ± SD atlas-to-subject-to-atlas error was 1.267 ± .191 mm for the control subjects and 1.246 ± .248 mm for the alcoholics [$t(173) = .629$, $p = .53$]; for no single landmarks did the alcoholics have significantly larger error than the control subjects. For each subject, for each target we also applied a search algorithm over ±2, 1.875 mm voxels in native space to locate the maximum amplitude of the eigenvector perpendicular to the fiber orientation. This location became the final target for fiber tracking.

Neuropsychological Tests

Using the digit symbol (DS) subtest of the Wechsler Adult Intelligence Scale-Revised (WAIS-R) (55), participants were presented with 93 randomly assigned digits from 1 to 9, each in a box with a blank box below, and they filled in the blank box by pairing each digit with a symbol from a key displayed above the grid. The scores were the number of boxes correctly completed in 90 seconds (standard score), time to complete the entire grid (56), and an incidental recall of the symbols. Fine finger movement was tested by subjects turning a knurled post with the index finger and thumb of the right hand, then left hand, and then both hands as quickly as possible for two 30-second trials. The score was the average of the two trials per condition of unimanual and bimanual performance (57). Ataxia was assessed by the stand on one foot balance test from the Fregly-Graybiel Ataxia Battery (58).

Statistical Analysis

Hemisphere effects were assessed with repeated-measures analysis of variance (ANOVA) for laterality and group (alcoholics vs. control subjects) for each of the 10 bilateral fiber bundles using values for each DTI metric (FA, ADC, λL, and λT) and followed up with paired *t* tests for group differences in DTI metrics of individual bundles. Group (control subject vs. alcoholic) by sex effects were assessed with repeated-measures ANOVA for the fiber bundles using each DTI metric (FA, ADC, λL, and λT) followed by *t* tests. We predicted that alcoholics would have both lower FA and higher diffusivity than control subjects.

Associations between fiber tract metrics and demographic, alcohol use, or behavioral test performance within the combined group of alcoholic men and women or for each sex separately were tested with Pearson product-moment correlations (*r*) or Spearman rank order correlations where appropriate. We predicted that lower FA and higher diffusivity would correlate with poorer behavioral and neuropsychological test performance. For all tests, we applied family-wise Bonferroni correction for 10 bilateral fiber bundles and the fornix; *p* values ≤ .005 were considered significant in the predicted direction.

Results

Laterality Effects and Alcoholism

Analysis of variance tested group-by-hemisphere interactions in each bilateral fiber bundle. Significant group effects and hemisphere effects were found for 8 of 10 bundles (Table 1 and Supplement 1), but in no case was the group-by-hemisphere interaction significant with family-wise Bonferroni correction for significance. Thus, we found no evidence that alcoholism significantly altered any normal left-right asymmetry for a given bundle. Subsequent analyses combined values for FA or diffusivity from left and right hemispheres and were based on mean values.

Fiber Bundle Integrity and Alcoholism

To identify the effects of diagnosis and sex, DTI metrics from the fornix and each of the 10 bilateral fiber bundles were submitted to group-by-sex ANOVAs, the results of which are presented in Supplement 1.

The mean ± SE for FA values and visual depiction of the fiber bundles are presented in Figures 2, 3, and 4 and for ADC, λL, and λT in Figures 5 and 6. Significant group differences were identified in 6 of the 11 bundles: fornix, internal and external capsules, frontal forceps, superior cingulate bundle, and superior longitudinal fasciculus. Specifically, FA was low in the frontal forceps and superior cingulate bundle, and diffusivity measures

were higher in the alcoholic than control groups in all six bundles. Trends were present in occipital forceps and inferior cingulate bundle FA.

Although across all subjects the sex effect was significant for FA or diffusivity in six fiber bundles, only trends were evident in group-by-sex interactions and then only for two bundles: internal capsule λL and inferior longitudinal fasciculus ADC and λL. There, alcoholic men had disproportionately greater diffusivity than the other groups.

Other Contributors to White Matter Fiber Degradation

Regression analyses tested the hypotheses that among the combined group of alcoholic men and women, lower FA and higher diffusivity would correlate with older age, more lifetime alcohol consumption, a shorter period of sobriety, or lower than normal body mass (indicative of poor nutrition). Family-wise Bonferroni correction required $p = .01$ in the predicted direction to support these directional hypotheses.

Greater lifetime alcohol consumption, in the alcoholic men but not women, correlated significantly or at trend levels with lower FA in the internal capsule ($r = -.30$, $p = .0193$), frontal forceps ($r = -.36$, $p = .005$), occipital forceps ($r = -.46$, $p = .0002$), and superior longitudinal fasciculus ($r = -.42$, $p = .001$) and with higher ADC in the internal capsule ($r = .36$, $p = .0057$), external capsule ($r = .29$, $p = .0275$), frontal forceps ($r = .29$, $p = .0275$), and superior longitudinal fasciculus ($r = .36$, $p = .004$). These correlations were confirmed with nonparametric Spearman rank tests.

Given that the alcoholic women had been sober for about twice as long as the alcoholic men and that some men had drunk considerably more than any woman, we derived a subgroup of 40 men and 25 women who were matched in length of sobriety (91 days for the men and 103 days for the women), age (45 years for men, 46 years for women), and lifetime consumption of alcohol (557 kg for men, 517 kg for women. We tested the difference between men and women in regional FA and ADC in each fiber bundle. These *t* tests revealed a significant disadvantage of alcoholic women over men in FA of the internal capsule ($p = .0013$), inferior cingulate ($p = .0076$), superior longitudinal fasciculus ($p = .002$), cerebellar hemisphere ($p = .0032$), and pontocerebellar ($p = .0078$) bundles; women also had higher ADC than men in the two cerebellar systems (hemispheres $p = .0005$; pontocerebellar $p = .0203$). By contrast, alcoholic women had lower ADC than alcoholic men in the fornix ($p = .0158$) and inferior longitudinal fasciculus ($p = .0141$).

Relative to alcoholics who had never smoked ($n = 23$), current or past smokers ($n = 63$) had lower FA in the pontocerebellar [$t(84) = 2.16$, $p = .0336$] and cerebellar [$t(84) = 2.998$, $p = .0036$] fiber bundles and higher ADC in the occipital forceps [$t(84) = 2.316$, $p = .023$] and inferior cingulate bundle [$t(84) = 2.482$, $p = .0151$]. Alcoholic men and women were combined in this analysis because the few alcoholic women who had never smoked ($n = 4$) represented too small a group for smoking-by-sex analysis. Curiously, alcoholic smokers had lower ADC in fornix than nonsmokers [$t(84) = 3.231$, $p = .0018$].

Body mass index, which was lower in alcoholic women than alcoholic men, was negatively correlated with ADC in the external capsule ($r = -.44$, $p = .0023$), frontal forceps ($r = -.39$, $p = .0413$), inferior longitudinal fasciculus ($r = -.522$, $p = .0044$), and cerebellar hemispheres ($r = -.49$, $p = .0086$) in the women but showed no such correlation in the men.

Half of the alcohol sample had a prior history of substance abuse, most commonly cocaine. Women were as likely to be substance abusers as men. Substance-abusing alcoholics had lower FA in the pontocerebellar [$t(85) = 2.86$, $p = .005$] and cerebellar hemisphere [$t(85) = 2.59$, $p = .011$] bundles, greater ADC in the occipital forceps [$t(85) = 2.45$, $p = .016$], and

higher λL in the superior longitudinal fasciculus [$t(85) = 2.49$, $p = .015$] than nonsubstance-abusing alcoholics.

Cognitive and Motor Performance Associations with DTI Metrics

Group-by-sex ANOVA indicated that although in some cases, women performed better than men (digit symbol output and time to completion) and in other cases men performed better than women (fine finger movement output), in no case was the group-by-sex interaction significant. Significant group differences indicated that compared with control subjects, alcoholics showed deficits in balancing on one foot with eyes open [$F(1,161) = 33.934$, $p = .0001$] and closed [$F(1,161) = 51.956$, $p = .0001$], fine finger movement output for unimanual [$F(1,161) = 5.582$, $p = .0193$] and bimanual conditions [$F(1,161) = 5.281$, $p = .0228$], digit symbol traditional output score [$F(1,161) = 16.025$, $p = .0001$], and time for grid completion [$F(1,161) = 7.779$, $p = .0059$] but not on the unannounced recall test of the symbol [$F(1.16) = 1.25$, $p = .2653$].

Given the lack of significant group-by-sex interactions in performance, correlations were conducted on the combined group of alcoholic men and alcoholic women. Among alcoholics, greater lifetime alcohol consumption was associated with lower scores on the traditional digit symbol test ($r = -.33$, $p = .0022$; Rho = −.37, $p = .0008$), time for grid completion ($r = -.17$, $p = .1196$; Rho = −.30, $p = .0062$), and balancing with eyes open ($r = -.22$, $p = .0374$; Rho = −.21, $p = .0538$).

Correlations (Supplement 1) in the predicted direction meeting family-wise Bonferroni correction ($p \leq .01$) were present between digit symbol score and FA in the frontal and occipital forceps and ADC in the frontal forceps and internal and external capsule. Time to complete the digit symbol grid correlated with FA in the inferior cingulate bundle and ADC in the fornix, internal and external capsules, and frontal forceps. Fine finger movement output correlated with inferior cingulate FA, and balancing with eyes closed correlated with fornix ADC.

Discussion

Diffusion tensor imaging anisotropy and diffusivity measures derived from quantitative fiber tracking of selective fiber bundles enabled in vivo examination of the effect of chronic excessive alcohol consumption on the microstructural integrity of major fiber bundles. These data extend earlier reports of macrostructural and microstructural vulnerability of frontal regions to alcohol dependence by assessing FA of specific white matter tracts and bundles and three measures of diffusivity: ADC and its axial and radial components (28–31). Diffusion tensor imaging metrics differed in vulnerability to alcoholism at different locations and in associations with cognitive and motor performance. Given comparable detection capabilities across fiber bundles, these results support a regional pattern, rather than a uniform distribution, of white matter microstructural compromise and sparing in chronic alcoholism.

Fiber bundles showing the most consistent effect of alcohol across DTI metrics in both men and women were anterior (internal and external capsules, frontal forceps, and fornix) and superior (superior cingulate) association fibers. By contrast, posterior (occipital forceps) and inferior (inferior longitudinal fasciculus, pontocerebellar, cerebellar hemispheres) association and projection tracts were relatively spared. Thus, this fiber tracking survey revealed extensive but region-specific alcohol effects, more than were evident from region-of-interest analysis (e.g., 18) or voxel-based analysis (21).

Several studies of regional brain volumes suggest that women show a “telescoping” effect, in that they exhibit greater parenchymal shrinkage and ventricular enlargement than men despite shorter alcoholism durations and lower consumption rates (7–9,59,60) (reviewed in 61). The samples of alcoholic women we studied with MRI, however, have not shown marked brain volume abnormalities when compared with age- and gender-matched control subjects (11,12). Using microstructural measures, we previously reported greater FA deficits in the splenium of alcoholic men than women (18,20). The current data, based on quantitative fiber tracking, reveal that regardless of the presence of alcoholism, women had lower FA than men in internal and external capsules, inferior cingulate bundle, and pontocerebellar and cerebellar hemisphere bundles and higher diffusivity in these and three additional regions: fornix, occipital forceps, and inferior longitudinal fasciculus. These sex-based differences suggest that women are at enhanced risk for alcoholism-related degradation in these areas.

Consideration of alcohol consumption variables revealed that greater lifetime alcohol consumption was predictive of more extensive fiber bundle degradation in the internal and external capsules and frontal and occipital forceps. This relationship, however, was limited to alcoholic men. The alcoholic women drank about half the amount of alcohol over their lifetimes relative to the alcoholic men, and this difference may have limited the range of values and attenuated possible correlations. Further, the alcoholic women were sober on average about 6 months, whereas the alcoholic men were sober for only 3 months. Thus, women may have had the advantage of some recovery between last drink and our examination. Although length of sobriety did not correlate with DTI metrics in men, women, or the combined alcoholic group, our analysis using groups matched in length of sobriety did reveal sex differences but not simply in favor of the men. Alcoholic women had lower FA than alcoholic men in internal capsule, inferior cingulate, superior longitudinal fasciculus, cerebellar hemisphere, and pontocerebellar bundles, whereas alcoholic women had lower ADC than alcoholic men in the fornix and inferior longitudinal fasciculus. In previous longitudinal studies measuring white matter volume change with abstinence, extent of recovery has not always been related to total lifetime consumption of alcohol (62–65).

Body mass index can be considered an index of nutritional ill health, both in the direction of obesity and malnourishment. Very low body weight can have implications for the condition of the brain, including white matter volume (66). Even though none of the alcoholic women herein were anorexic (lowest BMI = 18.1), lower BMI did relate to higher diffusivity in the external capsule, frontal forceps, inferior longitudinal fasciculus, and cerebellar hemisphere and perhaps put alcoholic women with lower BMI at greater risk for white matter microstructural abnormalities than those with a higher BMI.

Smoking was associated with poorer fiber bundle integrity of the pontocerebellar and cerebellum hemisphere bundles, a finding that should be considered in the context of a recent report of reduced gray matter but not white matter volume, albeit not microstructure, in smokers compared with nonsmokers (e.g., 67). Cognitive and motor functions, too, were associated with integrity of local fiber bundles. That any performance relations were detected is support for the functional meaningfulness of the focal DTI fiber tracking metrics indicates likely substrates for recovery of brain function with repair of alcoholism-damaged white matter constituents (cf., 62–64).

The hypothesis that alcohol has a more deleterious effect on the right than left hemisphere (68,69) received no support from this study. Yet, another recent report using a voxel-based analysis (21) noted lower FA in alcoholics than control subjects in right hemisphere frontal lobe regions identified with voxel-based morphometry but not in contralateral left hemisphere regions. However, sample size (15 alcoholics, 15 control subjects),

heterogeneity in sobriety length (5.7 ± 10 years, range .1–28 years), and the hypothesis-driven regional focus analysis of that study limit the conclusions drawn about the right hemisphere hypothesis of alcoholism.

Postmortem examination of chronic alcoholics indicates marked effects on brain white matter (70,71), disruption of its cytoskeletal integrity (72,73), and modification of protein expression (74). These pathological features may reduce intracellular structural complexity, making it less obstructive to water movement detectable with DTI. Further, supratentorial and infratentorial white matter fibers sustain demyelination (75,76), microtubule disruption (70,73,77–79), and axonal deletion with chronic alcoholism, possibly arising from regional neuronal loss (70,80–86). Diffusion tensor imaging revealed in vivo signs of demyelination, indexed by abnormally high radial diffusivity, a putative marker of impaired myelin integrity. In vivo DTI characterization of white matter microstructure of low anisotropy and high diffusivity in alcohol-dependent men and women described herein and elsewhere (13,18–20,87) is consistent with the postmortem signs and provides convergent validity for DTI metrics as in vivo markers of white matter neuropathology with a possible predilection for myelin disruption.

Acknowledgments

This work was supported by the National Institute on Alcohol Abuse and Alcoholism (AA005965, AA010723, AA17347, and AA012388).

We thank our research assistants (Jeffrey Eisen, Donna Murray, Marya Schulte, Andrea Spadoni, Carla Raassi, Daniel J. Pfefferbaum, Ted Sullivan, Alexander Jack, Julia Sandler, and Carrie McCloskey) and research clinicians (Stephanie A, Sassoon, Ph.D., Anne O'Reilly, Ph.D., and AnjaliDeshmukh, Ph.D.) for their work in subject recruitment, clinical evaluation, medical examination, scheduling, screening, data collection, and data entry.

References

1. Jernigan TL, Butters N, DiTraglia G, Schafer K, Smith T, Irwin M, et al. Reduced cerebral grey matter observed in alcoholics using magnetic resonance imaging. Alcohol Clin Exp Res. 1991; 15:418–427. [PubMed: 1877728]
2. Fein G, Dl Sclafani V, Cardenas VA, Goldmann H, Tolou-Shams M, Meyerhoff DJ. Cortical gray matter loss in treatment-naive alcohol dependent individuals. Alcohol Clin Exp Res. 2002; 26:558–564. [PubMed: 11981133]
3. Gazdzinski S, Durazzo TC, Studholme C, Song E, Banys P, Meyerhoff DJ. Quantitative brain MRI in alcohol dependence: Preliminary evidence for effects of concurrent chronic cigarette smoking on regional brain volumes. Alcohol Clin Exp Res. 2005; 29:1484–1495. [PubMed: 16131857]
4. Cardenas VA, Studholme C, Meyerhoff DJ, Song E, Weiner MW. Chronic active heavy drinking and family history of problem drinking modulate regional brain tissue volumes. Psychiatry Res. 2005; 138:115–130. [PubMed: 15766635]
5. Pfefferbaum A, Lim KO, Zipursky RB, Mathalon DH, Rosenbloom MJ, Lane B, et al. Brain gray and white matter volume loss accelerates with aging in chronic alcoholics: A quantitative MRI study. Alcohol Clin Exp Res. 1992; 16:1078–1089. [PubMed: 1471762]
6. Chanraud S, Martelli C, Delain F, Kostogianni N, Douaud G, Aubin HJ, et al. Brain morphometry and cognitive performance in detoxified alcohol-dependents with preserved psychosocial functioning. Neuropsychopharmacology. 2007; 32:429–438. [PubMed: 17047671]
7. Mann KF, Ackermann K, Croissan B, Mundle G, Diehl A. Neuroimaging of gender differences In alcoholism: Are women more vulnerable? Alcohol Clin Exp Res. 2005; 29:896–901. [PubMed: 15897736]
8. Hommer DW, Momenan R, Kaiser E, Rawlings RR. Evidence for a gender-related effect of alcoholism on brain volumes. Am J Psychiatry. 2001; 158:198–204. [PubMed: 11156801]
9. Hommer D, Momenan R, Rawlings R, Ragan P, Williams W, Rio D, et al. Decreased corpus callosum size among alcoholic women. Arch Neurol. 1996; 53:359–363. [PubMed: 8929159]

10. Agartz I, Momenan R, Rawlings RR, Kerich MJ, Hommer DW. Hippocampal volume in patients with alcohol dependence. Arch Gen Psychiatry. 1999; 56:356–363. [PubMed: 10197833]
11. Pfefferbaum A, Rosenbloom MJ, Deshmukh A, Sullivan EV. Sex differences in the effects of alcohol on brain structure. Am J Psychiatry. 2001; 158:188–197. [PubMed: 11156800]
12. Pfefferbaum A, Rosenbloom MJ, Serventi K, Sullivan EV. Corpus callosum, pons and cortical white matter in alcoholic women. Alcohol Clin Exp Res. 2002; 26:400–405. [PubMed: 11923595]
13. Pfefferbaum A, Adalsteinsson E, Sullivan EV. Dysmorphology and microstructural degradation of the corpus callosum: Interaction of age and alcoholism. Neurobiol Aging. 2006; 27:994–1009. [PubMed: 15964101]
14. Estruch R, Nicolas JM, Salamero M, Aragon C, Sacanella E, Fernandez-Sola J, et al. Atrophy of the corpus callosum in chronic alcoholism. J Neurol Sci. 1997; 146:145–151. [PubMed: 9077511]
15. Sullivan EV, Pfefferbaum A. Magnetic resonance relaxometry reveals central pontine abnormalities in clinically asymptomatic alcoholic men. Alcohol Clin Exp Res. 2001; 25:1206–1212. [PubMed: 11505052]
16. Sullivan EV, Deshmukh A, De Rosa E, Rosenbloom MJ, Pfefferbaum A. Striatal and forebrain nuclei volumes: Contribution to motor function and working memory deficits in alcoholism. Biol Psychiatry. 2005; 57:768–776. [PubMed: 15820234]
17. Bloomer CW, Langleben DD, Meyerhoff DJ. Magnetic resonance detects brainstem changes in chronic, active heavy drinkers. Psychiatry Res. 2004; 132:209–218. [PubMed: 15664792]
18. Pfefferbaum A, Sullivan EV. Microstructural but not macrostructural disruption of white matter in women with chronic alcoholism. Neuroimage. 2002; 15:708–718. [PubMed: 11848714]
19. Pfefferbaum A, Sullivan EV, Hedehus M, Adalsteinsson E, Lim KO, Moseley M. In vivo detection and functional correlates of white matter microstructural disruption in chronic alcoholism. Alcohol Clin Exp Res. 2000; 24:1214–1221. [PubMed: 10968660]
20. Pfefferbaum A, Adalsteinsson E, Sullivan EV. Supratentorial profile of white matter microstructural integrity in recovering alcoholic men and women. Biol Psychiatry. 2006; 59:364–372. [PubMed: 16125148]
21. Harris GJ, Jaffin SK, Hodge SM, Kennedy DN, Caviness VS, Marinkovic K, et al. Frontal white matter and cingulum diffusion tensor imaging deficits in alcoholism. Alcohol Clin Exp Res. 2008; 32:1001–1013. [PubMed: 18422840]
22. Xu D, Mori S, Solaiyappan M, van Zijl PC, Davatzikos C. A framework for callosal fiber distribution analysis. Neuroimage. 2002; 17:1131–1143. [PubMed: 12414255]
23. Lehericy S, Ducros M, Van de Moortele PF, Francois C, Thivard L, Poupon C, et al. Diffusion tensor fiber tracking shows distinct corticostriatal circuits in humans. Ann Neurol. 2004; 55:522–529. [PubMed: 15048891]
24. Stieltjes B, Kaufmann WE, van Zijl PC, Fredericksen K, Pearlson GD, Solaiyappan M, et al. Diffusion tensor imaging and axonal tracking in the human brainstem. Neuroimage. 2001; 14:723–735. [PubMed: 11506544]
25. Gerig, G.; Corouge, I.; Vachet, C.; Krlshnan, KR.; MacFall, JR. Quantitative analysis of diffusion properties of white matter fiber tracts: A validation study. Proceedings of the International Society for Magnetic Resonance in Medicine 13th Scientific Meeting; May 7–13; Miami, Florida. Berkeley, California: ISMRM; 2005. Abstract no. 1337
26. Sullivan EV, Adalsteinsson E, Pfefferbaum A. Selective age-related degradation of anterior callosal fiber bundles quantified in vivo with fiber tracking. Cereb Cortex. 2006; 16:1030–1039. [PubMed: 16207932]
27. Chanraud S, Reynaud M, Wessa M, Penttila J, Kostogianni N, Cachia A, et al. Diffusion tensor tractography in mesencephalic bundles: Relation to mental flexibility in detoxified alcohol-dependent subject. Neuropsychopharmacology. 2008 [published online ahead of print July 9].
28. Sun SW, Liang HF, Le TQ, Armstrong RC, Cross AH, Song SK. Differential sensitivity of in vivo and ex vivo diffusion tensor imaging to evolving optic nerve injury in mice with retinal ischemia. Neuroimage. 2006; 32:1195–1204. [PubMed: 16797189]
29. Sun SW, Liang HF, Trinkaus K, Cross AH, Armstrong RC, Song SK. Noninvasive detection of cuprizone induced axonal damage and demyelination in the mouse corpus callosum. Magn Reson Med. 2006; 55:302–308. [PubMed: 16408263]

30. Song SK, Sun SW, Ramsbottom MJ, Chang C, Russell J, Cross AH. Dysmyelination revealed through MRI as increased radial (but unchanged axial) diffusion of water. Neuroimage. 2002; 17:1429–1436. [PubMed: 12414282]
31. Song SK, Yoshino J, Le TQ, Lin SJ, Sun SW, Cross AH, et al. Demyelination increases radial diffusivity in corpus callosum of mouse brain. Neuroimage. 2005; 26:132–140. [PubMed: 15862213]
32. Arfanakis K, Haughton VM, Carew JD, Rogers BP, Dempsey RJ, Meyerand ME. Diffusion tensor MR imaging in diffuse axonal injury. Am J Neuroradiol. 2002; 23:794–802. [PubMed: 12006280]
33. Schulte T, Sullivan EV, Müller-Oehring EM, Adalsteinsson E, Pfefferbaum A. Corpus callosal microstructural integrity influences interhemispheric processing: A diffusion tensor imaging study. Cereb Cortex. 2005; 15:1384–1392. [PubMed: 15635059]
34. Pfefferbaum A, Rosenbloom MJ, Rohlfing T, Adalsteinsson E, Kemper CA, Dereslnski S, et al. Contribution of alcoholism to brain dysmorphology in HIV infection: Effects on the ventricles and corpus callosum. Neuroimage. 2006; 33:239–251. [PubMed: 16877010]
35. Pfefferbaum A, Rosenbloom MJ, Adalsteinsson E, Sullivan EV. Diffusion tensor imaging with quantitative fiber tracking in HIV infection and alcoholism comorbidity: Synergistic white matter damage. Brain. 2007; 130:48–64. [PubMed: 16959813]
36. Schulte T, Müller-Oehring EM, Pfefferbaum A, Sullivan EV. Callosal compromise differentially affects conflict processing and attentional allocation in alcoholism, HIV infection, and their comorbidity. Brain Imaging Behav. 2008; 2:27–38. [PubMed: 19360136]
37. Rosenbloom MJ, O'Reilly A, Sassoon SA, Sullivan EV, Pfefferbaum A. Persistent cognitive deficits in community-treated alcoholic men and women volunteering for research: Limited contribution from psychiatric comorbidity. J Stud Alcohol. 2005; 66:254–265. [PubMed: 15957677]
38. Rosenbloom MJ, Sullivan EV, Sassoon SA, O'Reilly A, Fama R, Kemper CA, et al. Alcoholism, HIV infection and their comorbidity: Factors affecting self-rated health-related quality of life. J Stud Alcohol Drugs. 2007; 68:115–125. [PubMed: 17149525]
39. Sullivan EV, Rohlfing T, Pfefferbaum A. Quantitative fiber tracking of lateral and interhemispheric white matter systems in normal aging: Relations to timed performance. Neurobiol Aging. 2008 [published online ahead of print May 19].
40. First, MB.; Spitzer, RL.; Gibbon, M.; Williams, JBW. Structured Clinical Interview for DSM-IV Axis/Disorders (SCID) Version 2.0. New York: Biometrics Research Department, New York State Psychiatric Institute; 1998.
41. Endicott J, Spitzer RL, Fleiss JL, Cohen J. The global assessment scale. A procedure for measuring overall severity of psychiatric disturbance. Arch Gen Psychiatry. 1976; 33:766–771. [PubMed: 938196]
42. Skinner, HA. Development and Validation of a Lifetime Alcohol Consumption Assessment Procedure. Toronto: Addiction Research Foundation; 1982.
43. Skinner HA, Sheu WJ. Reliability of alcohol use indices: The lifetime drinking history and the MAST. J Stud Alcohol. 1982; 43:1157–1170. [PubMed: 7182675]
44. Beck, AT.; Steer, RA.; Brown, GK. Manual for the Beck Depression Inventory-II. San Antonio, TX: Psychological Corporation; 1996.
45. Hollingshead, A.; Redlich, F. Social Class and Mental Illness. New York: John Wiley and Sons; 1958.
46. Crovitz HF, Zener KA. Group test for assessing hand and eye dominance. Am J Psychol. 1962; 75:271–276. [PubMed: 13882420]
47. Neeman M, Freyer JP, Sillerud LO. A simple method for obtaining cross-term-free images for diffusion anisotropy studies in NMR micro-imaging. Magn Reson Med. 1991; 21:138–143. [PubMed: 1943671]
48. Smith S. Fast robust automated brain extraction. Hum Brain Mapp. 2002; 17:143–155. [PubMed: 12391568]
49. Woods RP, Grafton ST, Holmes CJ, Cherry SR, Mazziotta JC. Automated image registration: I. General methods and intrasubject, intramodallty validation. J Comput Assist Tomogr. 1998; 22:139–152. [PubMed: 9448779]

50. Learned-Miller EG. Data driven image models through continuous joint alignment. IEEE Trans Pattern Anal Mach Intell. 2006; 28:236–250. [PubMed: 16468620]
51. Rohlfing T, Maurer CR. Nonrigid image registration in shared-memory multiprocessor environments with application to brains, breasts, and bees. IEEE Trans Inf Technol Biomed. 2003; 7:16–25. [PubMed: 12670015]
52. Rohlfing, T.; Brandt, R.; Maurer, JCR.; Menzel, R. Bee brains, B-splines and computational democracy: Generating an average shape atlas. In: Staib, L., editor. Proceedings of the IEEE Workshop on Mathematical Methods in Biomedical Image Analysis. Washington, DC: IEEE Computer Society; 2001. p. 187-194.
53. Rueckert D, Sonoda LI, Hayes C, Hill DL, Leach MO, Hawkes DJ. Nonrigid registration using free-form deformations: Application to breast MR images. IEEE Trans Med Imaging. 1999; 18:712–721. [PubMed: 10534053]
54. Morl S, Crain BJ, Chacko VP, van Zijl PC. Three-dimensional tracking of axonal projections in the brain by magnetic resonance imaging. Ann Neurol. 1999; 45:265–269. [PubMed: 9989633]
55. Wechsler, D. Wechsler Adult Intelligence Scale-Revised. San Antonio, TX: The Psychological Corporation; 1981.
56. Sassoon SA, Fama R, Rosenbloom MJ, O'Reilly A, Pfefferbaum A, Sullivan EV. Component cognitive and motor processes of the Digit Symbol Test: Differential deficits in alcoholism, HIV infection and their comorbidity. Alcohol Clin Exp Res. 2007; 31:1315–1324. [PubMed: 17550370]
57. Corkin, S.; Growdon, JH.; Sullivan, EV.; Nissen, MJ.; Huff, FJ. Assessing treatment effects from a neuropsychological perspective. In: Poon, L., editor. Handbook of Clinical Memory Assessment in Older Adults. Washington, DC: American Psychological Association; 1986. p. 156-167.
58. Fregly AR, Graybiel A, Smith MS. Walk on floor eyes closed (WOFEC): A new addition to an ataxia test battery. Aerosp Med. 1972; 43:395–399. [PubMed: 5045439]
59. Mann K, Batra A, Gunthner A, Schroth G. Do women develop alcoholic brain damage more readily than men. Alcohol Clin Exp Res. 1992; 16:1052–1056. [PubMed: 1471759]
60. Jacobson R. The contributions of sex and drinking history to the CT brain scan changes in alcoholics. Psychol Med. 1986; 16:547–549. [PubMed: 3763773]
61. Hommer DW. Male and female sensitive to alcohol-induced brain damage. Alcohol Res Health. 2003; 27:181–185. [PubMed: 15303629]
62. Shear PK, Jernigan TL, Butters N. Volumetric magnetic resonance imaging quantification of longitudinal brain changes in abstinent alcoholics. Alcohol Clin Exp Res. 1994; 18:172–176. [PubMed: 8198216]
63. Pfefferbaum A, Sullivan EV, Mathalon DH, Shear PK, Rosenbloom MJ, Lim KO. Longitudinal changes in magnetic resonance imaging brain volumes in abstinent and relapsed alcoholics. Alcohol Clin Exp Res. 1995; 19:1177–1191. [PubMed: 8561288]
64. O'Neill J, Cardenas VA, Meyerhoff DJ. Effects of abstinence on the brain: Quantitative magnetic resonance imaging and magnetic resonance spectroscopic imaging in chronic alcohol abuse. Alcohol Clin Exp Res. 2001; 25:1673–1682. [PubMed: 11707642]
65. Cardenas VA, Studholme C, Gazdzinskl S, Durazzo TC, Meyerhoff DJ. Deformation-based morphometry of brain changes in alcohol dependence and abstinence. Neuroimage. 2007; 34:879–887. [PubMed: 17127079]
66. Katzman DK, Zipursky RB, Lambe EK, Mikulis DJ. A longitudinal magnetic resonance imaging study of brain changes in adolescents with anorexia nervosa. Arch Pediatr Adolesc Med. 1997; 151:793–797. [PubMed: 9265880]
67. Durazzo TC, Cardenas VA, Studholme C, Weiner MW, Meyerhoff DJ. Non-treatment-seeking heavy drinkers: Effects of chronic cigarette smoking on brain structure. Drug Alcohol Depend. 2007; 87:76–82. [PubMed: 16950573]
68. Oscar-Berman M, Marinkovic K. Alcohol: Effects on neurobehavioral functions and the brain. Neuropsychol Rev. 2007; 17:239–257. [PubMed: 17874302]
69. Ellis RJ, Oscar-Berman M. Alcoholism, aging, and functional cerebral asymmetries. Psychol Bull. 1989; 106:128–147. [PubMed: 2667007]
70. De la Monte SM. Disproportionate atrophy of cerebral white matter in chronic alcoholics. Arch Neurol. 1988; 45:990–992. [PubMed: 3415529]

71. Harper C, Dixon G, Sheedy D, Garrick T. Neuropathological alterations in alcoholic brains. Studies arising from the New South Wales Tissue Resource Centre. Prog Neuropsychopharmacol Biol Psychiatry. 2003; 27:951–961. [PubMed: 14499312]
72. Harper C. The neuropathology of alcohol-specific brain damage, or does alcohol damage the brain? J Neuropathol Exp Neurol. 1998; 57:101–110. [PubMed: 9600202]
73. Putzke J, De Beun R, Schreiber R, De Vry J, Toile T, Zieglgansberger W, et al. Long-term alcohol self-administration and alcohol withdrawal differentially modulate microtubule-associated protein 2 (MAP2) gene expression in the rat brain. Brain Res Mol Brain Res. 1998; 62:196–205. [PubMed: 9813323]
74. Kashem MA, Harper C, Matsumoto I. Differential protein expression in the corpus callosum (genu) of human alcoholics. Neurochem Int. 2008; 53:1–11. [PubMed: 18513832]
75. Lewohl J, Wang L, Miles M, Zhang L, Dodd P, Harris R. Gene expression in human alcoholism: Microarray analysis of frontal cortex. Alcohol Clin Exp Res. 2000; 24:1873–1882. [PubMed: 11141048]
76. Tarnowska-Dziduszko E, Bertrand E, Szpak G. Morphological changes in the corpus callosum in chronic alcoholism. Folia Neuropathol. 1995; 33:25–29. [PubMed: 8673416]
77. Mayfield RD, Lewohl JM, Dodd PR, Herlihy A, Liu J, Harris RA. Patterns of gene expression are altered in the frontal and motor cortices of human alcoholics. J Neurochem. 2002; 81:802–813. [PubMed: 12065639]
78. Wiggins RC, Gorman A, Rolsten C, Samorajski T, Ballinger WE, Freund G. Effects of aging and alcohol on the biochemical composition of histologically normal human brain. Metab Brain Dis. 1988; 3:67–80. [PubMed: 3211076]
79. Paula-Barbosa MM, Tavares MA. Long term alcohol consumption induces microtubular changes in the adult rat cerebellar cortex. Brain Res. 1985; 339:195–199. [PubMed: 4040788]
80. Harper C, Kril J. If you drink your brain will shrink: Neuropathological considerations. Alcohol Alcohol Suppl. 1991; 1:375–380. [PubMed: 1845566]
81. Harper, CG.; Kril, JJ. Neuropathological changes in alcoholics. In: Hunt, WA.; Nixon, SJ., editors. Alcohol Induced Brain Damage: NIAAA Research Monograph No 22. Rockville, MD: National Institutes of Health; 1993. p. 39-69.
82. Lancaster, FE. Ethanol and white matter damage in the brain. In: Hunt, WA.; Nixon, SJ., editors. Alcohol-Induced Brain Damage: NIAAA Research Monograph No 22. Rockville, MD: National Institutes of Health; 1993. p. 387-399.
83. Badsberg-Jensen G, Pakkenberg B. Do alcoholics drink their neurons away? Lancet. 1993; 342:1201–1204. [PubMed: 7901529]
84. Alling C, Bostrom K. Demyelination of the mamillary bodies in alcoholism. A combined morphological and biochemical study. Acta Neuropathol. 1980; 50:77–80. [PubMed: 6769291]
85. Courville, CB. Effects of Alcohol on the Nervous System of Man. Los Angeles: San Lucas Press; 1955.
86. Kril JJ, Halliday GM, Svoboda MD, Cartwright H. The cerebral cortex is damaged in chronic alcoholics. Neuroscience. 1997; 79:983–998. [PubMed: 9219961]
87. Pfefferbaum A, Sullivan EV. Disruption of brain white matter microstructure by excessive intracellular and extracellular fluid in alcoholism: Evidence from diffusion tensor imaging. Neuropsychopharmacology. 2005; 30:423–432. [PubMed: 15562292]

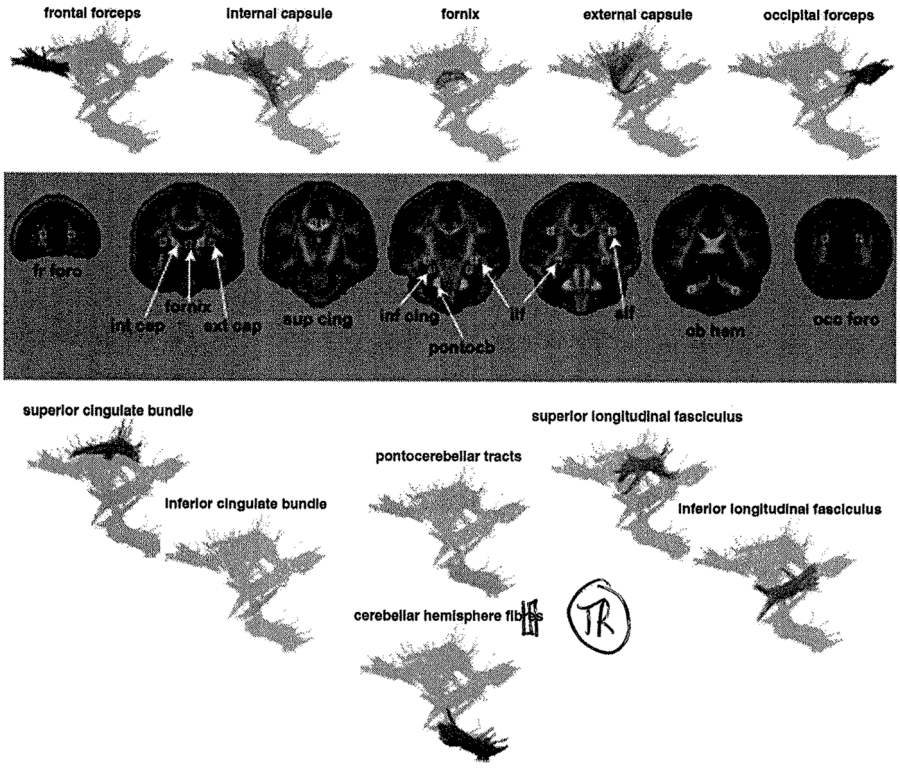

Figure 1.

DTI target locations for the fornix and 10 bilateral fiber bundles identified on coronal images of the population-average FA template and representative colorized fiber bundles superimposed on a composite sagittal image of all fiber bundles. For each subject, the targets and sources were mapped from the population FA template to that subject's native image space and passed to the fiber tracking routine. DTI, diffusion tensor imaging; FA, fractional anisotropy.

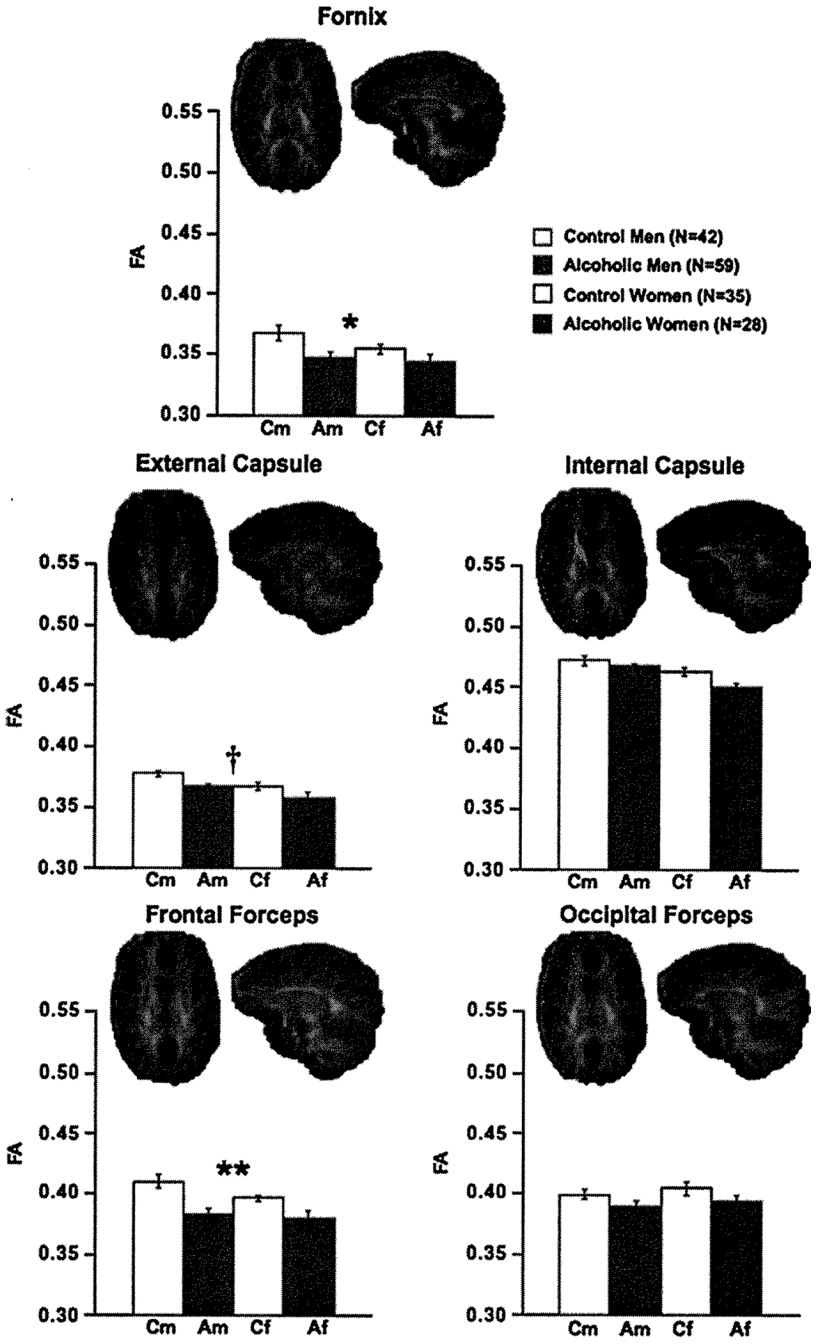

Figure 2.

Mean ± SE FA of the control men and women and alcoholic men and women for fornix, internal and external capsules, and frontal and occipital forceps fiber bundles, depicted above In axial and sagittal views. ANOVA group effects: †$p \leq .01$, *$p \leq .005$, **$p \leq .001$. Af, alcoholic female; Am, alcoholic male; ANOVA, analysis of variance; Cf, control female; Cm, control male; FA, fractional anisotropy.

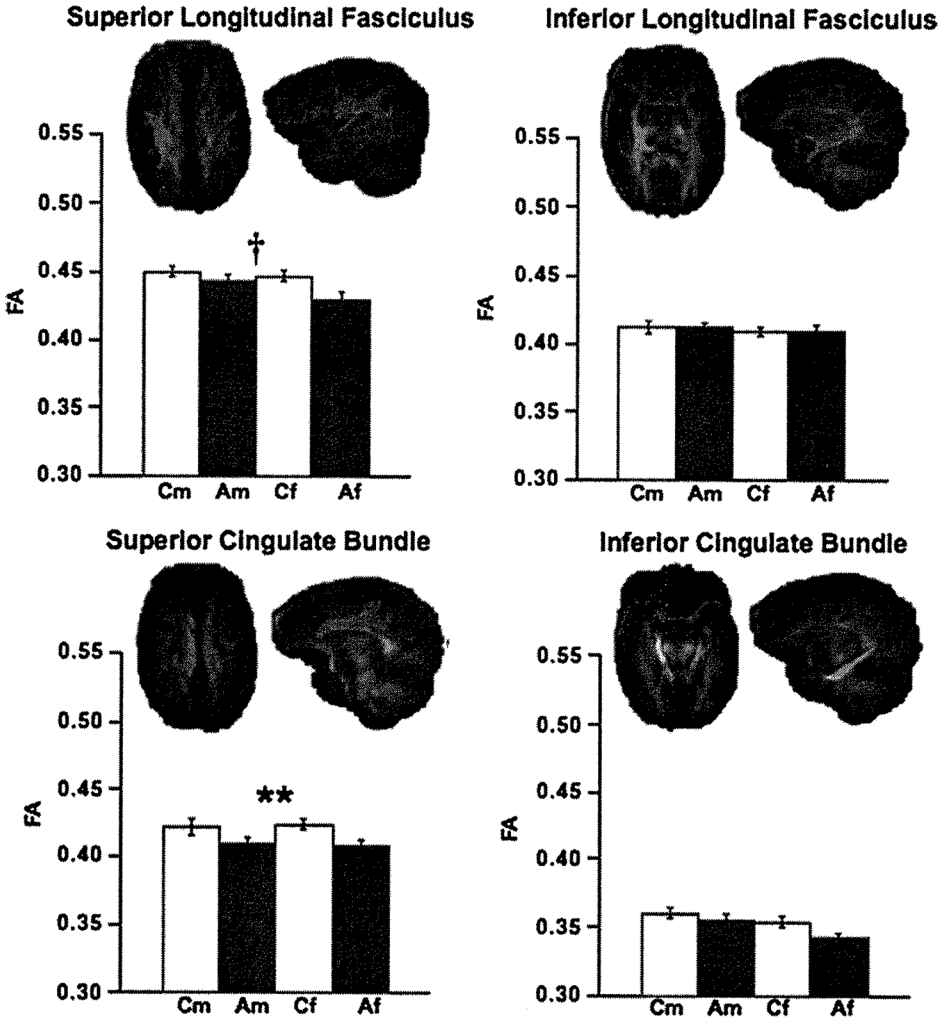

Figure 3.

Mean ± SE FA of the control men and women and alcoholic men and women for superior and inferior longitudinal fasciculus and superior and inferior cingulate fiber bundles, depicted above In axial and sagittal views. ANOVA group effects: †p ≤ .01, *$p \leq .005$, **$p \leq .001$. Af, alcoholic female; Am, alcoholic male; ANOVA, analysis of variance; Cf, control female; Cm, control male; FA, fractional anisotropy.

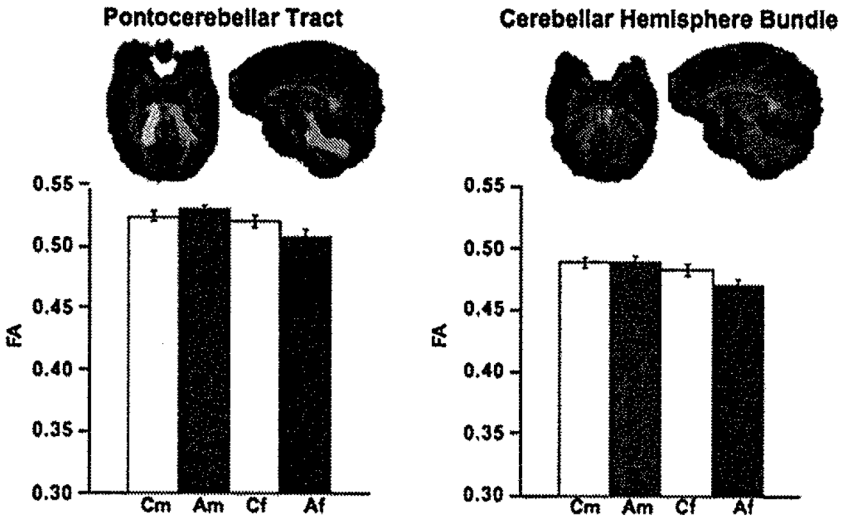

Figure 4.
Mean ± SE FA of the control men and women and alcoholic men and women for pontocerebellar tract and cerebellar hemisphere fiber bundle, depicted above in axial and sagittal views. Af, alcoholic female; Am, alcoholic male; Cf, control female; Cm, control male; FA, fractional anisotropy.

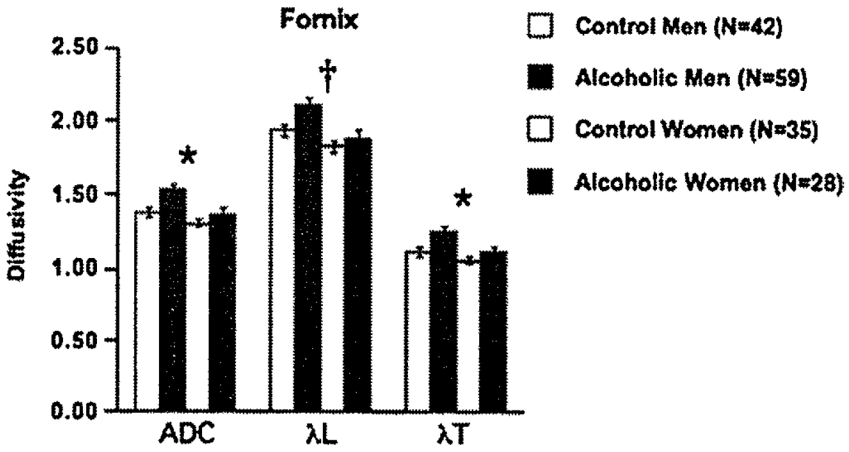

Figure 5.

Mean ± SE ADC, λL, and λT of the control men and women and alcoholic men and women for the fornix. ANOVA group effects: †$p \leq 01$, *$p \leq .005$. ADC, apparent diffusion coefficient; ANOVA, analysis of variance; λL, longitudinal diffusivity; λT, transverse diffusivity.

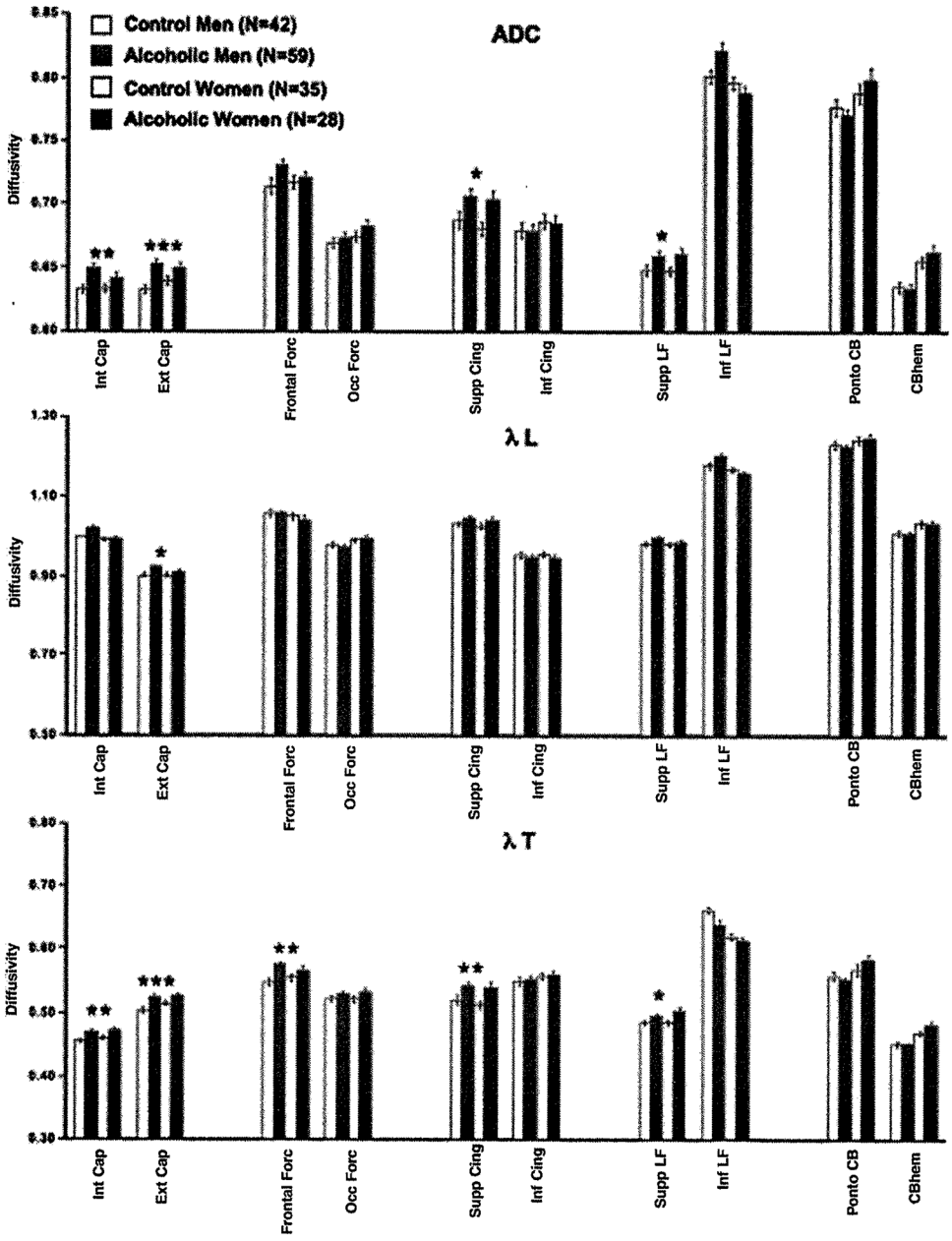

Figure 6.

Mean ± SE ADC, λL, and λT of the control men and women and alcoholic men and women for the 10 bilateral fiber bundles. ANOVA group effects: *p ≤.005, ***p* ≤.001, ****p* ≤.0001. ADC, apparent diffusion coefficient; ANOVA, analysis of variance; λL, longitudinal diffusivity; λT, transverse diffusivity.

Table 1

Demographic and Clinical Characteristics of Study Participants

	Alcoholic Men		Alcoholic Women		Control Men		Control Women		Group by Sex ANOVA							
									Group		Sex		Group × Sex		Group × Sex	
	Mean	SD	Mean	SD	Mean	SD	Mean	SD	*F*	*P*	F	*P*	*F*	*P*	χ^2	*P*
Men/Women	59		28		42		35								4.234	.0112
Age (years)	47.0	9.7	45.8	7.5	42.4	10.6	46.5	9.0	1.712	.1925	.933	.3355	3.289	.0715	—	—
Socioeconomic Status[a]	30.1	14.3	32.0	10.8	26.1	14.8	26.8	11.4	4.578	.0339	.393	.5314	.074	.7859	—	—
Years of Education	14.3	2.4	14.0	2.0	16.1	2.4	15.6	2.3	21.002	.0001	1.227	.2695	.050	.8237	—	—
Handedness (Crovitz)[b]	26.7	15.8	25.2	2.6	24.1	11.4	24.4	15.7	.538	.4644	.067	.7967	.153	.6959	—	—
Body Mass Index	26.9	4.0	24.4	4.7	26.9	4.7	24.9	4.6	.114	.7365	9.701	.0022	.133	.7155	—	—
Global Assessment of Functioning	54.1	11.5	59.0	10.8	10.3	2.2	6.4	1.5	144.761	.0001	5.620	.0200	.000	.9985	—	—
Beck Depression Index-II Score[c]	8.9	8.8	11.5	6.7	2.3	2.7	2.9	3.1	38.155	.0001	1.584	.2111	.675	.4135	—	—
Lifetime Alcohol (kg)	1005.0	111.9	536.1	73.4	61.0	78.7	25.5	31.2	76.258	.0001	9.171	.0028	6.770	.0101	—	—
Length Sober (days)	88.0	94.4	168.6	227.5	—	—	—	—	—	—	5.4760	.0216	—	—	—	—
Age Onset Alcohol Dependence	28.0	9.6	28.9	9.8	—	—	—	—	—	—	.1430	.7063	—	—	—	—
History of substance abuse/No History	29/30		14/14												.0	.9411
Days Since Used Drugs	4146.0	3624.0	20825	2239.0											3.8	.0563
Smoker/Nonsmoker[d]	39/19	—	24/4	—	11/26	—	9/33	—	—	—	—	—	—	—	40.973	.0001
Ethnicity (Caucasian/Minority)[e]	47/12	—	23/5	—	26/16	—	35/11	—	—	—	—	—	—	—	5.294	.1515

ANOVA, analysis of variance; BDI-II, Beck Depression Index-II.

[a] Hollingshead 2-factor score (higher score = lower status).

[b] Twelve alcoholics and 6 control subjects were left-handed (scored > 50).

[c] BDI-II not available from 14 alcoholic men, 10 alcoholic women, 16 control men, and 9 control women.

[d] Smoking history not available from 18 control subjects and 1 alcoholic.

[e] Caucasian non-Hispanic versus Hispanic plus other Minorities.